Prediction of post-sunset ESF based on the strength and asymmetry of EIA from ground based TEC measurements

S. V. Thampi, S. Ravindran, C. V. Devasia, T. K. Pant, P. Sreelatha and R. Sridharan

Space Physics Laboratory, Vikram Sarabhai Space Centre, Trivandrum-695 022, India

Abstract. The Coherent Radio Beacon Experiment (CRABEX) is aimed at investigating the equatorial ionospheric processes like the Equatorial Ionization Anomaly (EIA) and Equatorial Spread F (ESF) and their inter relationships. As a part of CRABEX program, a network of six stations covering the region from Trivandrum (8.5°N) to Nainital (29.3°N) is set up along the 77-78° E meridian. These ground receivers basically measure the slant Total Electron Content (TEC) along the line of sight from the Low Earth Orbiting satellites (NIMS). These simultaneous TEC measurements are inverted to obtain the tomographic image of the latitudinal distribution of electron densities in the meridional plane. In this paper, the tomographic images of the equatorial ionosphere along the 77-78°E meridian are presented. The crest intensities in the southern and northern hemispheres also show significant differences with seasons, showing the variability in the EIA asymmetry. The evening images give an indication of the prevailing electrodynamical conditions on different days, preceding the occurrence/non-occurrence of ESF. Apart from this, the single station TEC measurements from the Trivandrum station itself is used to estimate the EIA strength and asymmetry. Since this station is situated at the trough of the EIA, right over the dip equator, the latitudinal gradients on both northern (*N*) and southern (*S*) sides can be used to compute the EIA strength and asymmetry. These two parameters, obtained well ahead of the onset time of ESF, are shown to have a definite role on the subsequent ESF activity. Hence, both these factors are combined to define a new 'forecast parameter' for the generation of ESF. It has been shown that this parameter can uniquely define the state of the 'background ionosphere' conducive for the generation of ESF irregularities as early as 1600 IST. A critical value for the 'forecast parameter' has been identified such that when the estimated value for 'forecast parameter' exceeds it, the ESF is seen to occur. It is also observed that this critical value varies with season. All these aspects are studied in detail and the results are presented.

Index Terms. Equatorial ionisation anomaly, equatorial spread F, total electron content.

1. Introduction

The Indian Coherent Radio Beacon Experiment (CRABEX) has been initiated mainly to understand the large-scale processes over equatorial and low latitudes, like the Equatorial Ionization Anomaly (EIA) and Equatorial Spread F (ESF) and their inter-relationships. This experiment consists of six radio receivers stationed at Trivandrum (8.5°N, 77°E), Bangalore (13°N, 77.6°E), Hyderabad (17.3°N, 78.3°E), Bhopal (23.2°N, 77.2°E), Delhi (28.8°N, 77.2°E), and Nainital (29.3°N, 79.4°E) that are capable of receiving the 150 and 400 MHz beacon transmissions from the Low Earth Orbiting Satellites (LEOS). The satellites tracked are a part of the earlier Navy Navigational Satellite System (NNSS), now known as the Navy Ionospheric Monitoring System (NIMS). This receiver chain is unique as it covers the crest and trough regions of the EIA latitudinally, and goes well beyond the anomaly region. The simultaneous TEC data from all these stations are used to generate the tomographic maps at various local times, which represent the development of EIA.

The Equatorial Spread F (ESF) is a nighttime equatorial F-region ionospheric phenomenon, characterized by the presence of a wide spectrum of field-aligned irregularities generated due to a hierarchy of plasma instability processes. Since, the scintillations caused by these irregularities result in outages of the communication and navigation systems, understanding the variability of this phenomenon and forecasting /nowcasting the same are of considerable practical importance. The ESF is known to vary with season, local time, geographical location and solar activity, and over the years all these aspects have been studied extensively (Fejer and Kelley, 1980 and references therein). The theoretical foundation based on the Rayleigh-Taylor (R-T) instability mechanism (Haerendel, 1973) has been widely accepted. If seed perturbations are considered omnipresent, which is usually the case, the variability encountered by the phenomenon depends on the delicate balance of the background conditions and the operative forcing terms in the evening time equatorial F-region. The instability thus generated, is controlled by both ionospheric and neutral atmospheric parameters like plasma scale length (L), ion-neutral collision frequency (ν_{in}) and neutral winds in addition to the main driving force, viz. gravity. The generalized expression for the growth rate of the R-T instability in terms

of the various forcing parameters is (Sekar and Raghavarao, 1987; Kelley 1989).

$$\gamma = \frac{1}{L}\left[\frac{g}{\nu_{in}} + \frac{E_x}{B} + W_x\left(\frac{\nu_{in}}{\Omega_i}\right) - W_z\right] \quad (1)$$

where, E_x is the F-region zonal electric field, B is the geomagnetic field, Ω_i is the ion gyro frequency, W_x and W_z are the zonal and vertical winds respectively. It has been shown that for estimating the growth rate, the flux-tube integrated ionospheric conductivity should be taken into account (Kelly, 1989). Once triggered, the instability grows nonlinearly and the prevailing ionospheric conditions become important for its further development and sustenance.

The importance of ambient ionospheric and thermospheric conditions such as vertical plasma drifts, plasma density gradients, zonal, meridional and vertical neutral winds, initial seed perturbations etc., in the initiation and non-linear development of ESF and its dynamics has been well recognized (Sekar and Kelley, 1998). However, in a given season and solar epoch, under seemingly identical ionospheric conditions, ESF might occur on a day and might be absent on another.

The first indication of the significant role of the Equatorial Ionization Anomaly (EIA) intensification in the initiation of ESF was given by Raghavarao et al. (1988). They found that an intensification of the crest to trough ratio of the EIA in the 270 to 300 km altitude range between 1700 and 1900 LT occurred prior to ESF occurrence. Sridharan et al (1994) have followed it up and demonstrated that, there exists a precursor in the OI 630 nm dayglow that represented the EIA strength, which enables the prediction of ESF at least 3hours prior to its actual occurrence. Based on 13 days of observations, Mendillo et al. (2001) have pointed out that the best available precursor for pre-midnight ESF is the EIA strength at sunset and 85% successful 'forecasts' had been achieved. Anderson et al. (2004) showed that the scintillation activity is related to the maximum ExB drift velocity between 1830 and 1900 LT. All these results conclusively show that EIA and ESF are related. Recently, Devasia et al. (2002) provided the missing link between EIA and ESF through meridional winds. They showed that during the equinoctial months when the base height of the F layer (h'F) at 1900 IST was in the range of 270-300km, the meridional wind should be equatorward for ESF to occur over the equator. However, when h'F is >300km the ESF occurred irrespective of the polarity of the meridional wind. It was suggested that the observed equatorward winds could be an outcome of the pressure bulges associated with ETWA (Raghavarao et al., 1993), which in turn is linked to EIA (Devasia et al., 2002). All these studies demonstrate that the daytime electrodynamics play a decisive role in the initiation of ESF. As a consequence, various daytime electrodynamical parameters have been used in forecasting the ESF.

In this context, the present paper attempts to address this particular aspect of the day-to-day variability of the occurrence of ESF and also its deterministic forecasting. We are presenting the variabilities of EIA strength and asymmetry as observed in the ground based, single station Total Electron Content (TEC) measurements using radio beacon transmissions from LEOS, as well as the evening time tomographic images. The EIA strength and asymmetry factors observed at the time interval 1600-1845 IST have been uniquely combined to define a new threshold parameter for the generation of post sunset ESF.

2. Database

The Coherent Radio Beacon receivers (CRABEX receivers) located at Trivandrum (8.5°N, 77°E, Diplat. ~0.5°N), basically receives the two phase coherent signals 150 and 400 MHz transmissions from the NIMS satellites, and measures the differential Doppler between them. This is a part of the Coherent Radio Beacon Experiment (CRABEX), in which a chain of receivers along a 77-78°E meridian is being operated, for ionospheric tomography in the equatorial region. The days with Ap>12 have been omitted from the analysis, since the present attempt is to define the 'forecast parameter' for magnetically quiet time ESF activity. The ESF, in our study refers to the occurrence of bottom side spread F as seen by the co-located ground-based ionosonde at Trivandrum.

These slant path TECs estimated along a number of ray paths that define the passage of a LEO satellite from a chain of receivers are the basic data for the tomographic inversion. The inverse problem can be defined as

$$Y = Ax + E \quad (2)$$

where, Y is a vector of the observed TEC data, x is a vector of the unknown electron densities, and A is the geometry matrix, which describes the relationship between the received TEC data and the electron densities on each ray path. E represents the measurement and discretization errors.

In the present study, the Algebraic Reconstruction Technique (ART) is used for generating the electron density values. ART is a very simple iterative reconstruction technique, with a typical step,

$$\boldsymbol{x^{k+1} = x^k + \lambda_k \frac{y_i - \langle a^i, x^k \rangle}{\|a^i\|^2} a^i} \quad \textbf{(3)}$$

where x^k is the solution after k iterations, y is the data, a^i are the corresponding geometry elements and λ is the relaxation parameter.

Apart from the tomographic images of the EIA, to mathematically parameterize the relationship between the EIA parameters and the ESF, the TEC data from the Trivandrum station is used. Since the receiving station is situated at the trough of the EIA, right over the dip equator, the latitudinal gradients on both northern (N) and southern

(S) sides is a measure of the EIA strength. Using these, the strength of the anomaly (S_F) and the asymmetry in the anomaly (A_F) are defined as

$$S_F = \left(\frac{N+S}{2}\right) \quad and \quad A_F = \left(\frac{N-S}{(N+S)/2}\right) \tag{4}$$

It may be noted that all these definitions make use of only the latitudinal gradients and not the absolute TEC values. In the present analysis only those satellite passes with maximum off axis elevation > 50° are selected and for estimating the latitudinal gradients we have used only the part of the data for which the direct elevation angles are greater than 35°.

3. Results and discussion

Fig.1 shows a sample relative slant TEC data obtained at Trivandrum station and its projection to vertical. Simultaneous TEC records are obtained from the other stations also for reconstructing the tomographic image. The geocentric circular grids are used with a resolution of 50 km (lat) x 30 km (alt). The reconstruction is performed using ART. A sample tomographic image showing the presence of the EIA is shown in Fig. 2. The image is obtained for 28 September 2005, 1500 IST. The image clearly shows the presence of the northern crest of EIA at ~7° magnetic latitude. It can be seen that the EIA is weak and slightly asymmetric. The Ionosonde observation at Trivandrum shows that on this particular day there was no ESF.

To establish the relationship between EIA and ESF, we have used the TEC data from Trivandrum, for the period August 16- October 14, 2005. Tomographic maps are not available corresponding to all the days due to unavailability of data from other stations. Fig. 3 shows the northern and southern gradients calculated using the TEC data. It is clearly seen that the EIA is well developed after ~14:30 IST. As we know, the background ionospheric state is in turn manifested in the EIA characteristics, and hence to find the link between EIA and ESF, the TEC data in the time interval 1600-1845 IST is used. Fig. 4 shows the variation of EIA strength with day number. The red lines represent the ESF days and the blue lines represent the days without ESF. The black lines correspond to the days where ESF onset was after 2030 IST, i.e., delayed ESF, the usual time of the onset of ESF at Trivandrum being 1915-1945 IST. In the delayed ESF cases, the ESF observed at the site might be due to irregularities drifting into the field of view. In general, it is seen that the stronger EIA favors the generation of ESF in accordance with the earlier results cited in the previous section. However, it is clear that, taking the EIA strength alone, all ESF events cannot be 'predicted'. For example, on day numbers 241, 242 and 244, the EIA is nearly equally strong but ESF is present only on day number 242. This implies that forecasting ESF purely based on the strength of EIA alone is probabilistic in nature. Fig. 5 show the day-to-day variability of EIA asymmetry in the time interval 1600-1845 IST. From this, one could notice that stronger asymmetry seems to inhibit the ESF. However, there are days even when the EIA is significantly asymmetric, still ESF had occurred (for example day number 276 and 287). This only implies that EIA asymmetry alone does not suffice to make a deterministic forecast for the generation/suppression of ESF on a given day.

As mentioned earlier, the ESF occurrence or non-occurrence on a given day could be determined by the combined effect of the prevailing electrodynamical as well as the neutral dynamical conditions. The effects of these two independent aspects are manifested in the strength (S_F) and asymmetry (A_F) of the EIA, giving us an idea on the background conditions of the equatorial ionosphere in the evening hours. In other words, since the layer height at the post sunset hours bears a relation to the evening time S_F and A_F, we can combine these factors together in the form of a single parameter. A stronger EIA favors higher base height before the onset of ESF, whereas the stronger asymmetry brings it down. In short, $S_F \propto$ h'F and $A_F \propto$ (1/ h'F) and hence a Combined parameter (C) could be defined as

$$C = \sqrt{\frac{S_F}{A_F}} \tag{5}$$

One could see a clear demarcation wherein all the ESF days are having C > 2.35. This stands out in Fig. 6, which shows the variation of C with the day number. On days when C exceeds the threshold value of 2.35 ESF is seen to occur. Hence this new 'threshold parameter' is able to predict the ESF occurrence on a given day at a time much prior to its onset.

In the presence of seed perturbations, the background ionospheric conditions dictate whether the R-T instability could destabilize the equatorial F-region. The electrodynamics and the neutral dynamics during the course of the day set the stage for the post sunset ESF. The relation between the daytime EIA and the post sunset ESF (Raghavarao et al., 1988; Sridharan et al., 1994) and their possible linkage through meridional winds (Raghavarao et al., 1993; Devasia et al., 2002) only reiterate the complexities of the equatorial thermosphere ionosphere system. All the above studies though broadly refer the background conditions, do not attempt to bring out one single parameter, which could be used for forecasting the ESF well in advance. The present study makes use of the earlier knowledge and attempts towards accomplishing the same. The seasonal, solar activity and the longitudinal variability if any are to be studied in future with an expanded database.

4. Conclusion

The tomographic image showing the northern crest of the EIA is presented. The first systematic observations of EIA asymmetry as well as EIA strength are presented using latitudinal profiles of TEC obtained from a single ground

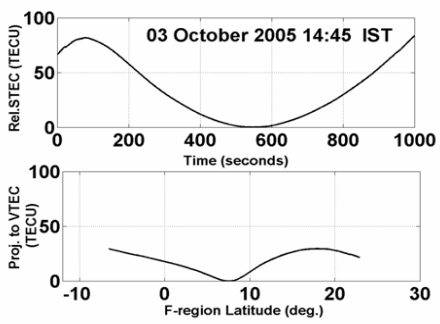

Fig. 1. An observed relative slant TEC data and its projection to the vertical plane. The data is from Trivandrum station.

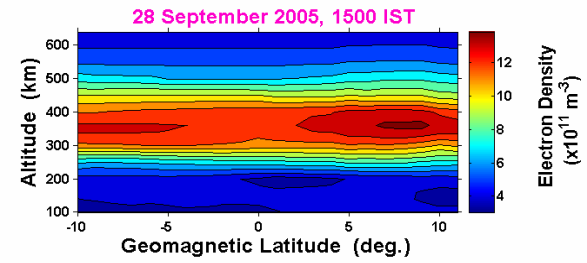

Fig. 2. The tomographic image showing the presence of northern crest of EIA.

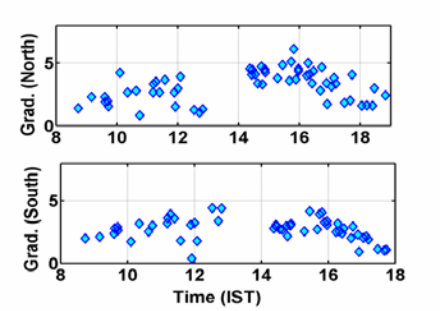

Fig. 3. The variation of northern and southern gradients with time.

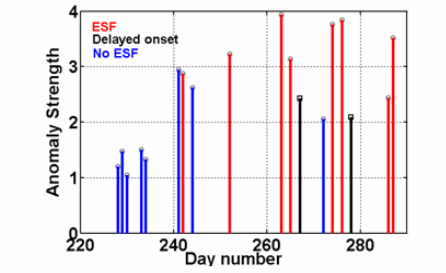

Fig. 4. The pattern of ESF occurrence/non occurrence with the EIA strength. The delayed onset corresponds to the ESF onset at Trivandrum after 20:30 IST.

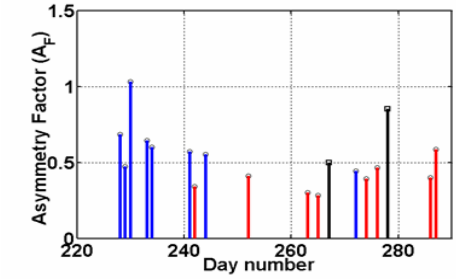

Fig. 5. The pattern of ESF occurrence/non occurrence with the EIA asymmetry.

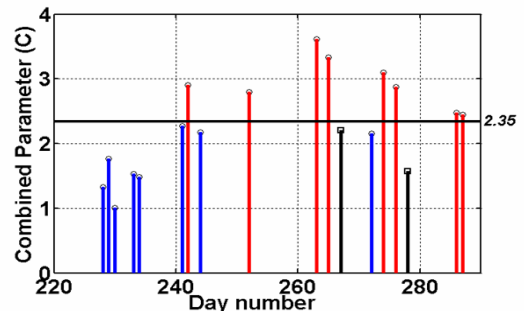

Fig. 6. The pattern of ESF occurrence/non occurrence with the newly defined combined parameter (C). It can be seen that for all the ESF days C >2.35.

based radio beacon receiver at Trivandrum. A combination of these values is used to arrive at a unique forecast parameter. That represents the background ionosphere so as to predict the occurrence of post sunset ESF as early as 1600-1845 IST. A critical value for the forecast parameter has been identified such that when the estimated value for 'C' exceeds it; the ESF is bound to occur. This new parameter defined in this study would be extremely important in understanding the enigma of the day-to-day variability of the occurrence/non-occurrence of ESF.

Acknowledgments: This work was supported by Department of Space, Government of India. One of the authors, SV Thampi, gratefully acknowledges the financial assistance provided by the Indian Space Research Organization through the research fellowship

References

D. N. Anderson, B. Reinisch, C. Valladare, J. Chau and O. Veliz, "Forecasting the occurrence of ionospheric scintillation activity in the equatorial ionosphere on a day-to-day basis", *J. Atmos. Sol. Terr. Phys.*, vol. 66, pp. 1567-1572, 2004.

C. V. Devasia, N. Jyoti, K. S. Viswanathan, K. S. V. Subbarao, D. Tiwari and R. Sridharan, "On the plausible linkage of thermospheric meridional winds with equatorial spread F", *J. Atmos. Sol. Terr. Phys.*, vol. 64, pp. 1-12, 2002.

B. G. Fejer and M. C. Kelley, "Ionospheric irregularities", *Rev. Geophys. and Space Phys.*, vol. 18, pp. 401-450, 1980.

G. Haerendel, *Theory of equatorial spread F*, unpublished report, Max Plank Institut fur Physik und astrophysik, Graching, Germany, 1973.

M. C. Kelley, *The earth's ionosphere: Plasma physics and electrodynamics*, Academic Press, San Diego, CA, 1989.

M. Mendillo, J. Meriwether and M. Biondi, "Testing the thermospheric neutral wind suppression mechanism for day-to-day variability of equatorial spread F", *J. Geophys. Res.*, vol. 106, pp. 3655-3663, 2001.

R. Raghavarao, M. Nageswararao, J. H. Sastri, G. D. Vyas and M. Sriramarao, "Role of equatorial ionization anomaly in the initiation of equatorial spread F", *J. Geophys. Res.*, vol. 93, pp. 5959-5964, 1988.

R. Raghavarao, W. R. Hoegy, N. W. Spencer and L. Wharton, "Neutral temperature anomaly in the equatorial thermosphere- A source of vertical winds", *Geophys. Res. Lett.*, vol. 20, pp. 1023-1026, 1993.

R. Sekar and M. C. Kelley, "On the combined effects of vertical shear and zonal electric field patterns on nonlinear equatorial spread F evolution", *J. Geophys. Res.*, vol. 103, pp. 20735-20748, 1998.

R. Sekar and R. Raghavarao, "Role of vertical winds on the Rayleigh-Taylor mode instabilities of the nighttime equatorial ionosphere", *J. Atmos. Terr. Phys.*, vol. 49, pp. 981-985, 1987.

R. Sridharan, D. Pallam Raju and R. Raghavarao, "Precursor to equatorial spread-F in OI 630.0 nm dayglow", *Geophys. Res. Lett.*, vol. 21, pp. 2797-2800, 1994.